

Technical Note

## Assessment of axial force effect on improved damage index of confined RC beam-column members

Reza Abbasnia<sup>1,\*</sup>, Neda Mirzadeh<sup>1</sup>, Kamyar Kildashti<sup>2</sup>

Received: July 2009 , Revised: September 2010, Accepted: April 2011

### Abstract

In recent years, different damage indexes have been introduced in engineering literature. The most prominent one among other counterparts is the 1985 Park and Ang's damage index ( $DI_{PA}$ ), which demonstrates well calibration against experimental results. Hence, it has traditionally had broad application in the field of structural engineering. Commonly, in  $DI_{PA}$  relevant parameters are assessed based on plastic-hinge approach, which is not well suited to consider the coupled response between stress resultants (axial force and flexural moment) especially in grossly nonlinear domain. The reason is that named approach is utilized constant shape plastic moment-curvature curve, which is not capable of varying the shape throughout loading history. Another drawback of plastic-hinge method is the difficulty of representing precisely partial yielding of the cross-section. To remedy the situation, the fiber discretization technique is used in this paper. Based on the fiber discretization strategy, not only have the stiffness and strength degradation been characterized more accurately, but also the distribution of plasticity along the plastic zone has been considered. Besides, the multi-directional effect of axial force and flexural moment is considered to assess  $DI$  parameters. Additionally, this strategy directly incorporates the effect of transverse confinement into cross sectional constitutive behaviour.

**Keywords:** Damage index, Fiber discretization, Multi-directional effect, Transverse confinement.

### 1. Introduction

Present design philosophy derived from demand reduction factor allows structures to be designed with lateral strength lower than that required to remain elastic when severe earthquakes take place. As a result, these structures are not capable to withstand seismic loading without some level of structural damage. In the aftermath of 1970's earthquakes, researchers have focused their attention on financial loss or humans' toll owing to structural damage. In this regard, several advances have been made in seismic code provisions to limit the amount of structural damage [1]. In technical literature, a large number of damage indexes ( $DI_s$ ) have been proposed [2], [3]. Some of them are based on cyclic fatigue concepts [4] and others make use of structural mode [5] in prediction of damage. Moreover, a group of damage indexes include ductility ratio or plastic deformation [6], [7], [8] whilst some concern hysteretic energy absorption [9], [10].

Typically, advanced damage indexes are not dependent on single parameter but they are integration of different parameters. For example, Park's and Ang's model [11], and Reinhorn's and Valles's model [12] consist of both deformation and energy terms. Also the model suggested by Colombo and Negro [13] is the function of strength, ductility and energy. Among all models, Park's and Ang's model ( $DI_{PA}$ ) is employed so widely in engineering applications. The reason lies behind both simplicity and extensive calibration against experimental results. The practical damage index should have the ability to quantify effective features in design such as axial load and confinement. In accordance with Kono and Watanabe [14] experiment, large axial load affects the length of the plastic zone and ultimate curvature capacity of concrete column that eventually leads to severe damage [15]. Unfortunately, some computational procedures due to using constant multi-linear force-deformation relations for different types of cross-sections, are not thoroughly able to consider the coupled response between axial load and flexural moment; hence they are likely that lead to erroneous results for prediction of damage index [16], [17]. A plenty of investigations have been devoted to incorporate axial load into measure of damage index [14], [18]. It is noteworthy that most

\* Corresponding Author: [abbasnia@iust.ac.ir](mailto:abbasnia@iust.ac.ir)  
1 Department of Civil Engineering, Iran University of Science and Technology, Tehran, Iran  
2 School of Civil Engineering, University of Tehran, Tehran, Iran

proposed strategies evaluate damage index without knowing the complete stress-strain and hysteretic energy history through dynamic analysis; hence, they are not able to include the effect of strong-motion duration. Besides the range of their applicability is evidently limited. To tackle the problem, in this paper  $DI_{PA}$  which includes both deformation and hysteretic terms is used. Then so-called fiber method is employed as an analysis oriented tool to assess axial load effect on damage index terms [16], [17]. It is interesting to note that fiber discretization approach is able to consider simultaneous effects of axial load and flexural moment in more accurate distribution of plasticity along the member length and cross sectional area. Also because material in terms of steel and concrete are defined as stress-strain constitutive behaviour in this approach, the transverse confinement effect as a key factor in concrete deformability could come into analytical procedures conveniently. It means that fiber discretization method is able to incorporate the amount of transverse confinement into demand terms as well as capacity terms of damage index. Several investigations have been proposed in literature to approximate experimental results on the basis of numerical formulations [19], [20], [21], [22]. Among all, Mander [22] relationship is well-established to characterize the effect of transverse confinement on concrete compressive strength and ultimate deformation based on smeared crack approach [16].

In this paper four principal stages are addressed:

(1) To verify the fibre method; first, a displacement controlled quasi-static history is performed for a column with pre-defined dimensions and characteristics, then the analytical results are compared to those of full-scale specimen tested in the laboratory.

(2) To calculate damage index based on fibre method, a one story frame is modelled and subjected to different earthquake ground motion records along with various axial loads. Overall, damage index consideration is classified base on tension or compression control regions of interaction diagram.

(3) The same frame with the ground motion earthquake causing maximum damage index is assigned to evaluate the confinement effect with the aid of Mander's formula.

(4) First, a four story frame is simulated and designed using current standards and codes. Then it is exerted to dynamic time history stimulation. Finally the damage index based on different formula is compared.

## 2. Hysteretic characteristics of beam-column element based on fiber approach

### 2.1. Verification of fiber-based software against experimental result

The computer program named SeismoStruct ver. 4.0.3 [23] performing the analyses on the basis of fiber discretization method is applied for analytical assessment. It is proper program to capture stiffness and strength degradation as well as distribution of plasticity. Moreover, Mander's model implemented in this software enables it to recognize confinement by entering confining coefficient.

To verify the results of this program, they are compared with

the experimental results of a circular column. This column was tested at the laboratories of the National Institute of Standards and Technology (NIST) [24]. The test was performed using a displacement controlled quasi-static history and axial load as shown in Figure 1 and Figure 2, respectively. The column was made of 36 MPa concrete and had modulus of elasticity of approximately 28300 MPa. Grade 60 steel with an actual yield stress of 475 MPa and elasticity modulus of 189200 MPa was used as longitudinal reinforcement. The cross-section in Figure 2 also shows the reinforcement details.

In comparison, Figure 3 indicates that the responses obtained from the analysis and results of tested column agree fairly well. For example maximum load attained in the analysis 1375 kN and 1379 kN (positive and negative) compare well with those observed in the test 1263 kN and 1317 kN, respectively.

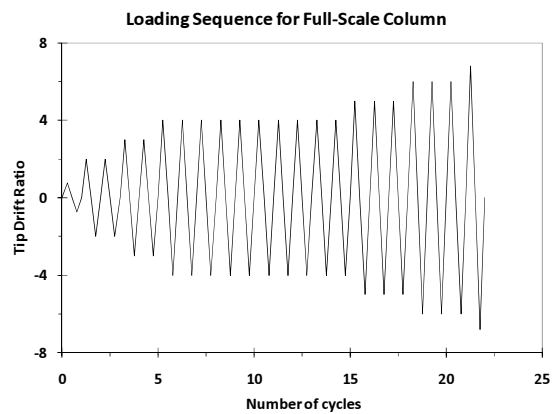


Fig. 1. Quasi-static history loading [21]

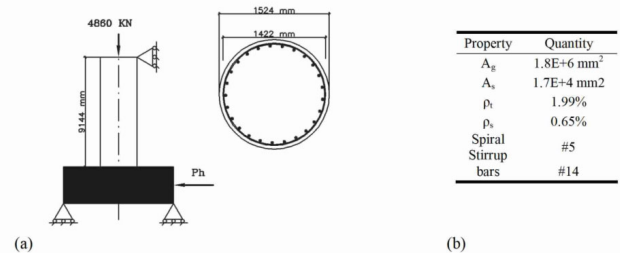


Fig. 2. (a) Geometry and axial load of tested specimen and (b) reinforcing characteristics [24]

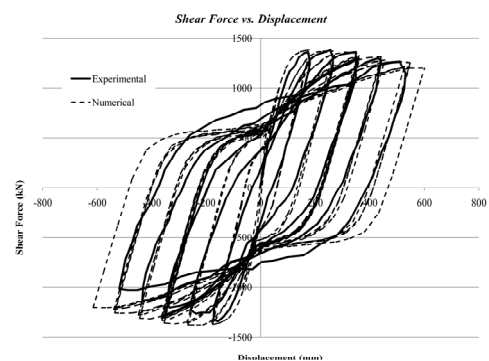


Fig. 3. Comparison between the experimental and the numerical response of column element [24]

## 2.2. Deterioration of strength and stiffness

In presence of axial load, strength and stiffness degradation of RC members become more significant. Fiber discretization concept by using the suitable material constitutive model efficiently describes the strength and stiffness degradation under severe cyclic histories. This matter is important to evaluate damage parameters more accurately. The specimen introduced in section 2.1 is subjected to two levels of axial force ( $P_b$ =balance axial force). As can be observed in Figure 4, by increasing the level of axial force the cyclic characteristics of member tends to drop down. Moreover, the slope of descending branch is visibly depends on axial load ratio. Thus, the fiber method is appropriate alternative compared for capturing of axial load and bending moment interaction.

## 3. AXIAL LOAD INFLUENCE ON DAMAGE INDEX

### 3.1. Tension-control region of interaction diagram

With the purpose of considering axial load, a one story frame including one bay is constructed. The geometrical configuration, element designation, dimensions and reinforcement details are shown in Figure 5. The model is made of concrete with maximum compressive strength of 40 MPa whose strain at peak stress is 0.002 mm/mm. For reinforcement, A706, grade 60 steel with yield strength of approximately 410 MPa and modulus of elasticity of 200000 MPa is used whose strain hardening ratio is 0.005. The Menegotto-Pinto's model [25], which has been implemented in

the program as the steel constitutive behaviour, is assigned for the longitudinal rebars. Furthermore, Mander's model [22] is of assistance for modeling of confined and unconfined concrete. Total floor dead load as well as 25% of live load is comprised the seismic mass, which is equal to 13100 kg for each column. This mass is lumped at top of each column. The model is subjected to some ground motion excitations (from PEER strong ground motion database record) listed in Table 1.

First, when there is not any axial load on frame,  $DI_{PA}$  is calculated based on the following equation:

$$DI_{PA} = \frac{\theta_{max} - \theta_r}{\theta_u - \theta_r} + \beta \frac{E_H}{E_{mon}} \quad (1)$$

Where  $\theta_{max}$  is the maximum rotation attained during the loading history;  $\theta_u$  is the ultimate rotation capacity of the section;  $\theta_r$  is the recoverable rotation when unloading takes place;  $E_H$  is the hysteretic energy in the section;  $E_{mon}$  is energy capacity under monotonically increasing deformation and  $\beta$  is a constant which depends on structural characteristics ( $\beta$  is assumed 0.15).

Since through the analytical process the distribution of plasticity is considered,  $\theta$  needs to be determined at the end of plastic zone length under seismic excitations. The program can measure the length of plastic zone by determining the summation of length of sub-element whose moment of Gauss points acquires yield moment. Similarly,  $\theta_u$  should be attained at the end of plastic zone of mentioned element when it is loaded monotonically by increasing lateral load. The total amount of input energy imparted into MDOF systems is

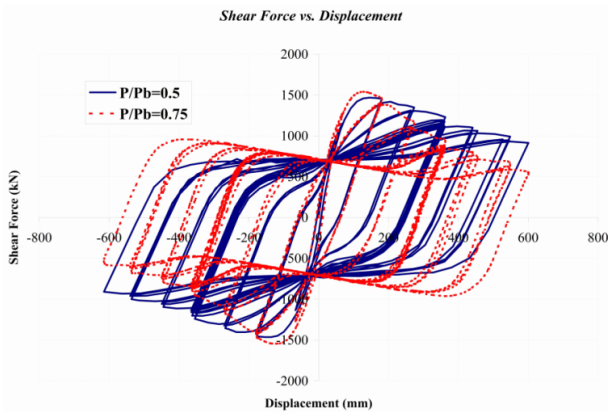


Fig. 4. Hysteretic behaviour of designated column for two levels of axial force

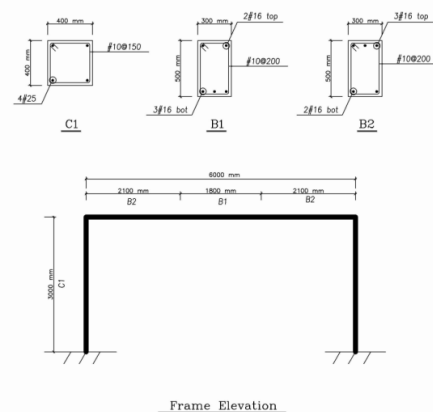


Fig. 5. Geometry and configuration of modeled frame

Table 1. Detail of records used for time history analysis

Date	Earthquake	Magnitude ( $M_s$ )	Station Name	Record/Component	PGA ( $cm/s^2$ )
17/01/94	Northridge	6.7	Newhall-Fire Station	NORTHR/NWH090	520
10/18/89	Loma Prieta	7.1	WAHO	LOMAP/WAH090	626
17/01/94	Northridge	6.7	Tarzana-Cedar Hill	NORTHR/TAR360	971
20/09/99	Chi-Chi	7.6	TCU084	CHICHI/TCU084-W	1138
16/01/95	Kobe	6.9	Takatori	KOBE/TAK000	604

calculated by integrating of governing differential equation of motion as follows:

$$\int_0^u \mathbf{m}\ddot{\mathbf{u}}(t)d\mathbf{u} + \int_0^u \mathbf{c}\dot{\mathbf{u}}(t)d\mathbf{u} + \int_0^u \mathbf{f}_s(\mathbf{u}, \dot{\mathbf{u}})d\mathbf{u} = -\int_0^u \mathbf{m}\ddot{\mathbf{u}}_g(t)d\mathbf{u} \quad (2)$$

where  $\mathbf{m}$  and  $\mathbf{c}$  are the mass and damping matrices, respectively.  $\mathbf{f}_s(\mathbf{u}, \dot{\mathbf{u}})$ ,  $\boldsymbol{\tau}$  and  $\mathbf{u}$  are the vector of resisting internal forces, the influence vector and the vector of generalized displacements, respectively.  $\ddot{\mathbf{u}}_g(t)$  is the earthquake input excitation.  $t$  is the duration when the hysteretic energy  $E_H$  would be calculated. Since for damage index calculation  $E_H$  at the end of record is required,  $t$  is equal to duration of earthquake. Additionally, hysteretic energy in Equation 2 is obtained based on following relation:

$$E_H(t) = \int_0^u \mathbf{f}_s(\mathbf{u}, \dot{\mathbf{u}})d\mathbf{u} - E_s(t) \quad (3)$$

where  $E_s(t)$  is the elastic energy. Since independent degree of freedom of Bernoulli-Euler beam element includes two end moments and one axial force, the hysteretic term of input energy in Equation 3 can be expressed as follows:

$$E_H(t) = \sum_{I,K} \int_0^\theta M(\theta, \dot{\theta})d\theta - E_s(t) \quad (4)$$

where  $M(\theta, \dot{\theta})$  is the end moments and "I", "K" are the indexes of end nodes. If  $\theta$  is substituted by  $t$  which is the orientation of Equation 4, the following relation will be obtained:

$$E_H = \sum_{I,K} \int_0^t M(\theta, \dot{\theta}) \frac{d\theta}{dt} dt - E_s(t) = \sum_{I,K} \int_0^t \dot{\theta} M(\theta, \dot{\theta}) dt - E_s(t) \quad (5)$$

Besides, monotonically increasing energy ( $E_{mon}$ ) can be obtained on the basis of the following equation:

$$E_{mon} = \int_0^{l_p} M d\theta = \int_0^{l_p} M \frac{d\theta}{dx} dx = \sum_{h=1}^{NG} M_h \frac{d\theta_h}{dx} |J| w_h \quad (6)$$

where  $l_p$  is the length of plastic zone,  $h$  denotes the monitored section,  $w_h$  is the corresponding weight factor,  $NG$  is the number of Gauss quadrature point,  $|J|$  is the Jacobean of transformation. In this report, the number of Gauss quadrature points is assumed "2", so the respective weight factor is "1" and  $|J|$  is  $l_p/2$ . It should be noted that if plastic zone length of an element is divided into several sub-elements,  $E_H$

and  $E_{mon}$  will be summation of hysteretic energy of each sub-element.

During the loading history, deformation term of  $DI_{PA}$  will be maximized if either  $\theta$  reaches its peak or  $\theta_u$  becomes minimal. Knowing axial load decreases ultimate curvature and consequently ultimate rotation ( $\theta_u$ ), a critical time step for computing  $DI_{PA}$  is step of maximum axial load. The influence of axial load ( $N$ = axial force &  $N_0$ = maximum axial capacity) on reduction of ultimate curvature is shown in Figure 6.

In next steps different axial loads are exerted to the frame and  $DI_{PA}$  is calculated. Before evaluation of damage index, capacity and demand terms of damage index need to be calculated. For this aim, capacity energy and  $\beta = 0.15$  of hysteretic energy versus axial load ratio as well as capacity and the plastic rotational demand are displayed in Figure 7(a) and Figure 7(b), respectively. As can be seen in Figure 7(b), totally the demand and capacity plastic rotation have downward trends when axial load enlarges; however, the rate of changes are not equal. Also, as can be seen in Figure 7(a) the similar trend is observed in capacity energy terms of  $DI_{PA}$ ; nevertheless the hysteretic energy does not necessarily descend with magnifying axial load. The reason is that based on Equation (6) flexural moment and rate of rotational variation simultaneously determine hysteretic energy. Amplifying axial load on one hand increases flexural moment, on the other hand decreases rotation of section. If less

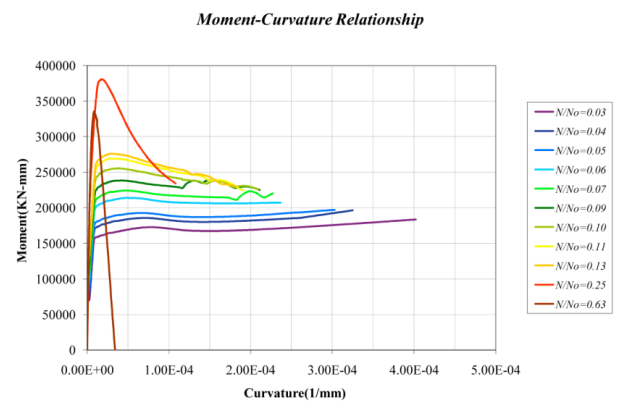


Fig. 6. Influence of axial load on descent of ultimate curvature

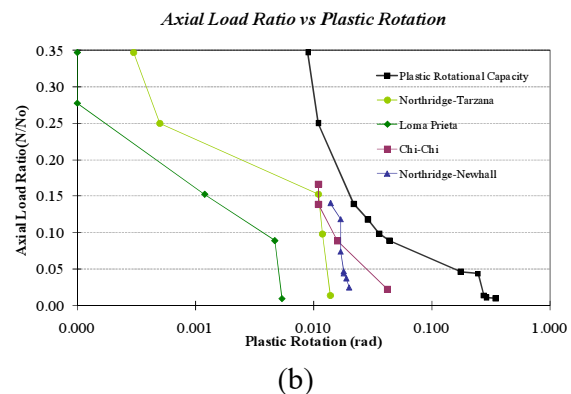
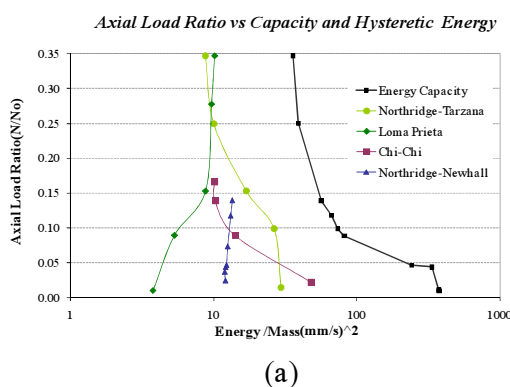


Fig. 7. (a) Influence of axial load on capacity and hysteretic energy; (b) Influence of axial load on reduction of rotational demand and capacity.



rotational variation than flexural moment increase is obtained, hysteretic energy is likely to decrease; otherwise energy absorption is going to exceed.

The damage index is in fact acquired by dividing previously calculated demand to capacity terms. Figure 8(a) to Figure 8(d) illustrates  $DI_{PA}$  versus axial force ratio of column for each earthquake record.

As can be observed in Figure 8, the deformation and hysteretic portion of total damage index is illustrated separately. It should be noted that before the failure occurs the combination of flexural moment and axial loads corresponding to each earthquake is located in tension control region of interaction diagram. As can be seen in Figure 8(a) to Figure 8(d), totally damage index enlarges with increasing axial load mainly due to reduction of capacity. As can be seen in Figure 8(a) to Figure 8(d), energy term of damage index has gradual progress owing to less deterioration of energy capacity than energy demand. Considering deformation term, mainly it has drastic increase. Figure 8(d) shows that axial load presence initially increases deformation damage then due to severe decline of rotation this term tends to achieve the zero value.

### 3.2. Compression-control region of interaction diagram

As can be seen in Figure 8(b) and Figure 8(d), when axial load is beyond the axial load ratio of 0.35 (balance axial load to maximum axial load capacity of section) element does not exhibit ductile behaviour. In fact, in compression control

region of interaction diagram due to brittle behaviour, sudden failure is expected. In addition, the brittle failure is so instantaneous that the computation of damage index is not feasible. In tension control region such as Figure 8(a) and Figure 8(c), although columns suffer high level of damage; the behaviour is not as brittle as compression region. This means that in compression control region of interaction diagram damage index remains zero unless the strength of section attains yield strength. So in this region an element can carry a wide range of flexural moments in cooperation with different axial loads but as soon as multi-axial action goes beyond yield strength sudden failure happens.

### 4. Confinement effect in damage index

Basically, to sustain lateral load due to seismic events, reinforced concrete elements are required to have enough axial strength and ductility. The enhancement in axial strength and ductility can be interpreted as confinement. As long as acceptable confinement is provided, damage level of reinforced concrete elements diminishes. To prove the point, the analytical investigation is conducted; first, Northridge-Newhall-FireStation record (whose damage on frame is maximum) is selected. In Figure 9 the influence of confinement on dwindling of total damage as well as hysteretic and deformation damage is represented. Afterwards, confining enhancement effect is evaluated when axial load presents in frame. In this study a model proposed by Mander

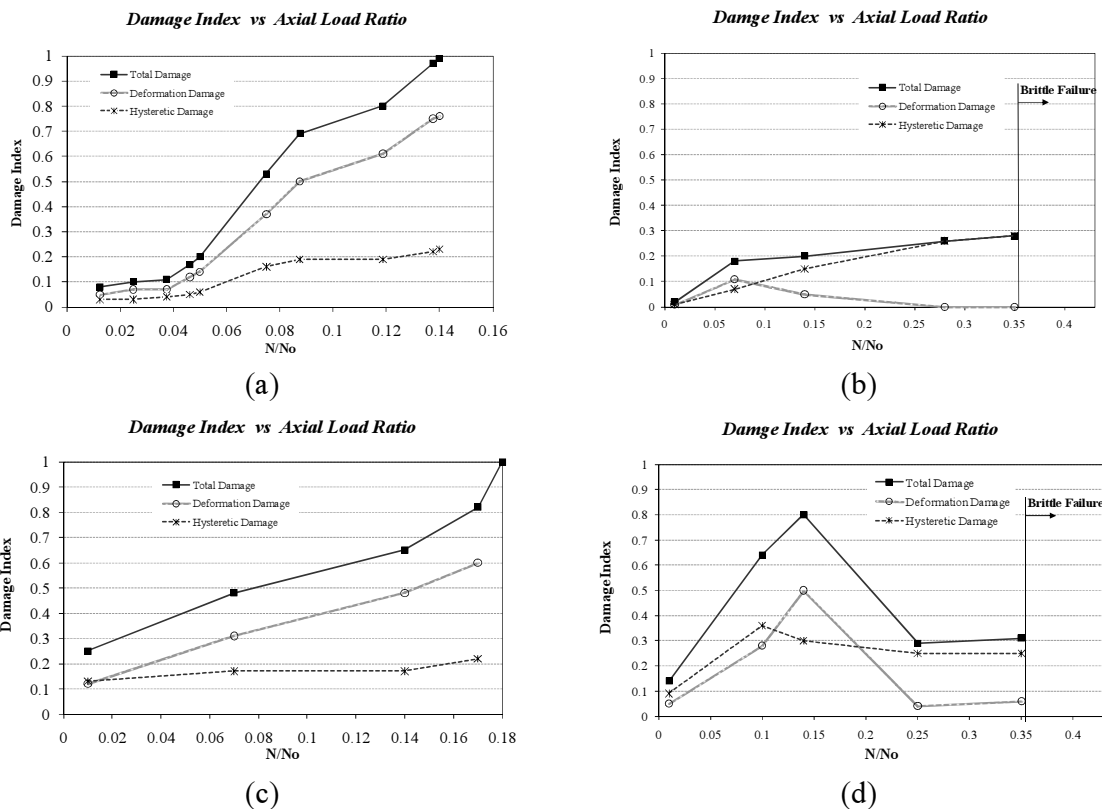


Fig. 8. Influence of axial load on damage index in four earthquake records; (a) Northridge-Newhall (b) Loma Prieta-Waho (c) Chi-Chi-TCU084 (d) Northridge-Tarzana

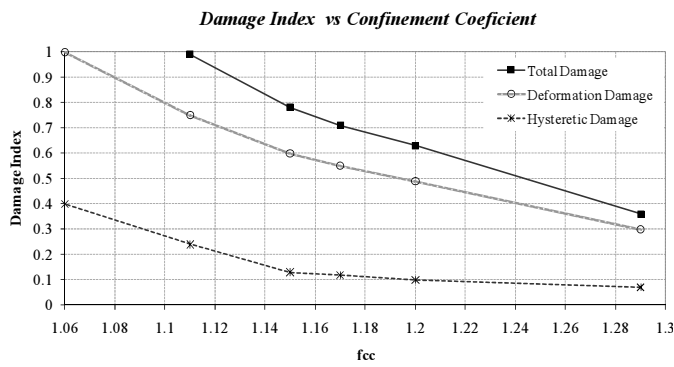


Fig. 9. Influence of Confinement on Damage Index during Northridge-Newhall Earthquake

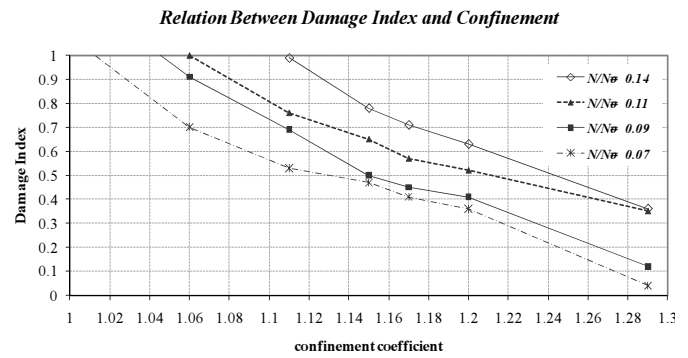


Fig. 10. Damage Index and Confinement Coefficient Relationship Based on Different Axial Load Ratio during Northridge-Newhall Earthquake

et al. considering the yield strength and arrangement of confining reinforcement to define compressive stress and strain of confined concrete is used. Mander's relations for square section are defined as follows:

$$f'_{lx} = K_e \rho_x f_{yh} \quad (7)$$

$$K_e = \frac{\left[ 1 - \sum_{i=1}^n \frac{w'_i{}^2}{6b_c^2} \right] \left( 1 - \frac{S'}{2b_c} \right)^2}{1 - \rho_{cc}} \quad (8)$$

$$f_{cc} = -6.83 f'_{lx}{}^2 + 6.83 f'_{lx} + 1 \quad (9)$$

$$f_{cc} = f'_{cc} / f'_{co}; f_{lx} = f'_{lx} / f'_{co} \quad (10)$$

Where  $f'_{lx}$  is the effective lateral confining pressure,  $f'_{co}$  is peak stress ratio for unconfined concrete,  $K_e$  is confining effectiveness coefficient,  $\rho_x$  is the ratio of transverse confining steel volume to confined concrete core volume,  $f_{yh}$  is the yield strength of transverse reinforcement,  $w'_i$  is the  $i$ th clear distance between adjacent longitudinal bars,  $b_c$  is core dimension to centrelines of hoop,  $S'$  is the clear

Table 2. Range of transverse reinforcement and confinement coefficient

Size and Space	$f_y$ (KN/mm <sup>2</sup> )	$\epsilon_{cu}$	$f_{cc}$
T12/200	0.4	0.018	1.1
T12/150	0.4	0.022	1.17
T12/125	0.4	0.024	1.22
T12/100	0.4	0.028	1.29
T10/200	0.4	0.014	1.07
T10/150	0.4	0.017	1.12
T10/125	0.4	0.019	1.15
T10/100	0.4	0.022	1.2
T10/75	0.4	0.026	1.29
T8/200	0.3	0.008	1.03
T8/150	0.3	0.009	1.06
T8/125	0.3	0.01	1.07
T8/100	0.3	0.011	1.1
T8/75	0.3	0.013	1.14

vertical spacing between hoops,  $\rho_{cc}$  is the ratio of the longitudinal reinforcement area to section core and  $f_{cc}$  is confinement coefficient and  $f'_{cc}$  is confined concrete strength. To estimate the confined concrete ultimate strain a simple and conservative equation is given by Priestley et al [27]:

$$\epsilon_{cu} = 0.004 + \frac{1.4 \rho_s f_{yh} \epsilon_{su}}{f'_{cc}} \quad (11)$$

Where  $\epsilon_{su}$  is steel strain at maximum tensile stress.  $\rho_s = 2\rho_x$  for square section. It is noted that Equation (10) can be used for a section in combined bending with axial compression. Utilizing above formulas,  $f_{cc}$  and  $\epsilon_{su}$  is obtained conveniently as essential input for the program. In order to simplify the process of finding  $f_{cc}$  and  $\epsilon_{su}$ , Table 2 is suggested by authors. This table intends to define mentioned parameters practically regarding the size and space and yield strength of rebars. For all rebars,  $\epsilon_{su}$  is equal to 0.14.

Figure 10 illustrates the relation between  $DI_{PA}$  and  $f_{cc}$  based on different axial load ratio. As can be observed,  $DI_{PA}$  reduces dramatically when confinement coefficient enhances for all axial ratios mainly owing to increase of deformation and energy capacity. Although for lower axial ratio contribution of confinement is more significant. For example, for  $N/N_0=0.07$  weak confinement leads to damage index more than 0.4 (repairing limit), while high confinement maintains damage even less than  $DI_{PA}=0.05$  (slight damage). In fact, with respect to Table 2., high confinement is feasible by applying #13@100 that provides confinement coefficient of 1.29. For column stated in compression control region, probably confining enhancement could not improve sudden failure of element but just shifts the point of failure on interaction diagram to point with larger strength.

## 5. Improving damage index

The results achieved by previous parts are beneficial to improve damage index in accordance with axial-flexural interaction. As discussed, since axial load significantly affects deformation and energy terms of damage index, a practical damage index should be affected by axial load. To take advantage of the  $DI_{PA}$  model as an index of structural damage, the axial load should be considered in damage terms. Thus, a

modification needs to be carried out based on the level of axial load over tension or compression control region of interaction diagram. In compression control region of interaction curve, as soon as the demand exceeds the design strength, damage index is equal to unity and calculation of damage index does not make any sense. However, until the demand does not reach the design strength the damage index is equal to zero. The improvement in damage index  $DI_1'$  and  $DI_2'$  for a generic RC beam-column member is introduced as follows:

$$\text{If } N < N_b \quad DI_1' = \max \left\{ \begin{array}{l} \frac{\theta_{max} - \theta_r}{\theta_u - \theta_r} + \beta \frac{E_H}{(E_{mon})_{\theta_{max}}} \\ \frac{\theta_n - \theta_r}{\theta_{u(min)} - \theta_r} + \beta \frac{E_H}{(E_{mon})_{\theta_n}} \end{array} \right. \quad (11)$$

$$\text{If } N \geq N_b \quad DI_2' = \begin{cases} 0 & ; \text{if } M < M_y \\ 1.0 & ; \text{if } M \geq M_y \end{cases}$$

Where  $N_b$  is the axial load related to balanced point in interaction diagram,  $\theta_{u(min)}$  is related to the time step when axial load is maximum,  $\theta_n$  and  $(E_{mon})_{\theta_n}$  is the rotation and monotonic energy of this time step, respectively,  $(E_{mon})_{\theta_{max}}$  is monotonic energy when  $\theta_{max}$  is reached.  $M_y$  is yield moment and  $M$  represents the moment of column. Other parameters were defined before. Since demand hysteretic energy is cumulative identity, it is constant in the first couple of relations.

## 6. Simulation of mdof system

This section mainly is devoted to assess proposed damage index of structures which have been design based on allowable confinement rate in current seismic codes and standards. Furthermore, participation of axial load makes the research more actual. For this purpose, first a four story frame is modelled. The model specification is reported in Table 3. The geometrical configuration, element designation, dimensions and reinforcement details are shown in Figure 11. The confinement rate for columns is a little more than minimum requirement of ACI (2005) however, for beams it is less than the recommended value. The structure is designed based on

Table 3. model specification

Material properties	ASTM standard
Loading pattern	ASCE 7-02
Design	ACI(2005) code
Distributed dead load on 2 first Beams	38 N/mm
Distributed dead load on 2 second Beams	36 N/mm
Distributed live load on Beams	30 N/mm
Column dead load	18.7 kN
Seismic mass(Floor dead load+0.25% of live load) of first and second story	15070 kg
Seismic mass(Floor dead load+0.25% of live load) of third and fourth story	14470&13530
Rayleigh damping ratio	5%
ground motion excitation	Kobe(Table1)

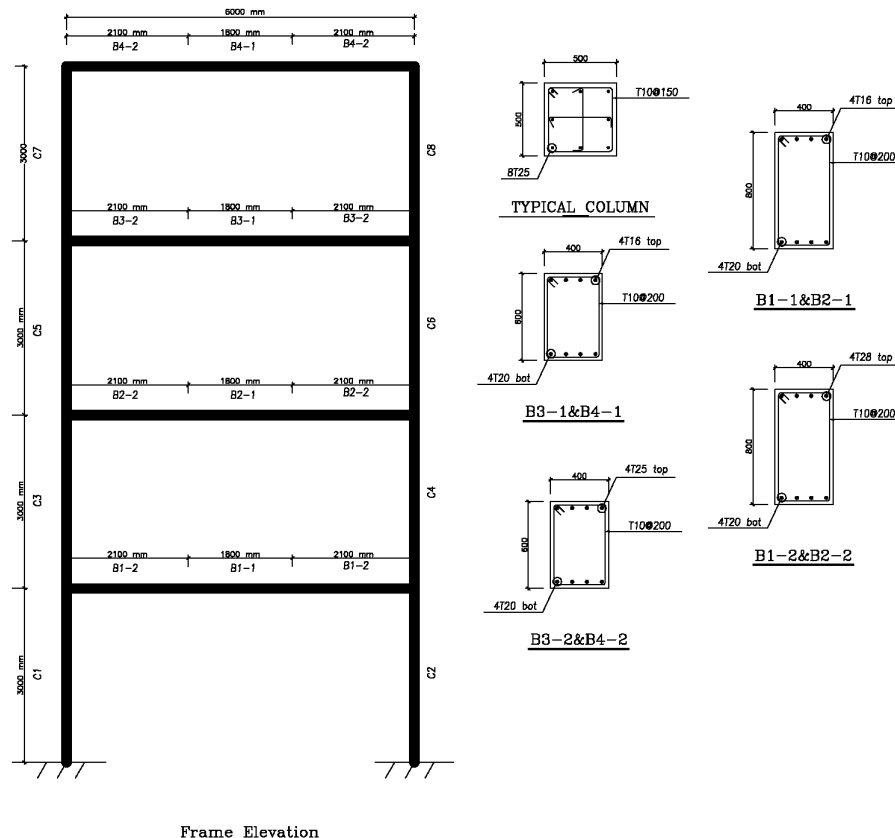


Fig. 11. Geometry and configuration of 4-story frame

**Table 4.** model specification

Element Name	Location	DI'(Hysteretic)	DI'(Deformation)	DI'(Hysteretic)	DI'(Deformation)	DI'(Total) <sub>max</sub>
		$\theta=\theta_{max}$	$\theta=\theta_{max}$	$\theta_h=(\theta_h)_{min}$	$\theta_h=(\theta_h)_{min}$	
C1	bot	0.43	1.78	0.55	0.82	2.21
	top	0.01	0.04	0.03	0.05	0.08
C2	bot	0.02	0.33	0.04	0.41	0.45
C3	top	0.04	0.2	0.04	0	0.24
B1	left(M+)	0.14	0.37	-	-	0.51
	left(M-)	0.12	0.01	-	-	0.13
	right(M+)	0.01	0.14	-	-	0.15
	right(M-)	0.12	0.09	-	-	0.21
B2	left(M+)	0.09	0.21	-	-	0.3
	left(M-)	0.07	0.01	-	-	0.08
	right(M+)	0.07	0.09	-	-	0.16
	right(M-)	0.08	0.07	-	-	0.15
B3	left(M+)	0.03	0.06	-	-	0.09
	left(M-)	0.02	0	-	-	0.02
	right(M+)	0.02	0.02	-	-	0.04
	right(M-)	0.03	0.08	-	-	0.11

occupancy important factor of 1, site class C, the spectral response acceleration at short periods ( $S_s$ ) 1.5g and at 1 second ( $S_1$ ) is 0.6g. The design is performed regarding Intermediate Reinforced Concrete Moment Frame. The reinforcement details and confinement arrangement follow of ACI (2005) seismic provision for intermediate moment frames.

The results of analysis for damaged elements are recorded in Table 4 where damage index is reported for couple of circumstances: first, the rotation of section is maximum; second, the axial load is maximum. In the last column of Table 4 the maximum value of two previous conditions is reported as total damage index. Accordingly, the maximum damage index belongs to the ground level of columns. It is noteworthy that in column C2 in contrast to C1 the maximum damage index is not appeared when rotation is maximum but it occurs when the axial load reaches the maximum. However, the rotation related to this damage index is noticeably less than maximum rotation. Moreover, another imperative outcome is that although the confinement for beams was provided less than recommended by ACI (2005) standard, their damage index is considerably less than that of columns. In fact, since usually beams have no axial force and are flexural-controlled solely, the confinement influence is less effective for them than columns. However,  $DI'$  of some beams are beyond the repair level. It seems that if the minimum requirements of standard were provided  $DI'$  would be negligible. In contrast, for columns confining effect appears to have an important influence on the progression of damage. Nevertheless, enhancing confining effect in

columns does not necessarily ensure the safety of them. The reason is that, sometimes axial-dominant behaviour of an element leads to severe damage even if high confinement is provided.

To ensure that the modified  $DI_{PA}$  which is evaluated based on fiber method, rather accurately estimates the level of damage, the result of C1 column is compared with three other damage indexes. First ASCE41-06 [1] model, second Reinhorn and Valles's model [12] and last IDARC Software [24]. The results reported in the following table:

Based on the criteria introduced in ASCE41-06 the effect of confinement is determined as a conforming or non-conforming situation, which depends on the amount of transverse confinement. In addition, the effect of axial load and shear force can be considered in terms of ductility capacity. The main drawback of this procedure is that the hysteretic energy effect is neglected. Additionally, the confinement effect cannot be assessed as quantitative parameters in estimation of damage index. Nevertheless, this code is quite acceptable criteria to assess the rate of damage in a particular element. The comparison between ASCE41-06 formulation and modified  $DI_{PA}$  model represents that since in ASCE41-06 just the deformation term presents, the damage is less than what reached by modified  $DI_{PA}$  model. However, it can be observed that based on ASCE41-06 as valid criteria the column is sustained the high level of damage. In Reinhorn & Valles's model although both terms of deformation and energy are included but due to restriction of hinge method the values are not as much as DIPA model. The value obtained by IDARC Software with hinge method suffers from the similar deficiency.

**Table 4.** model specification

Element Name	ASCE41-06	Reinhorn and Valles	IDARC Software	Modified Park and Ang
C1	1.43	2.11	0.60	2.21



In IDARC software, since there is no correlation between axial load and variation of ductility the results do not have enough accuracy.

## 6. Conclusion

The main conclusions reached by this paper can be fallen into the following parts:

1. The operation of axial in combination with flexural moment in damage index of section located beyond or below balance region in interaction diagram is principally different. For latter condition, axial load progresses damage index more due to reduction of capacity terms. However, sometimes influence of axial load on descending of demand response compensates reduction of capacity and consequently damage index decreases. In compression control region of interaction diagram, as far as yield strength is not attained, damage is not obtained whereas beyond this margin, increasing in axial load definitely leads to sudden failure of element.

2. Confining enhancement evidently helps to reduce damage index of flexural-dominant element mainly owing to increase of deformation and energy capacity. In contrast, for element with the governing axial load, confining enhancement dose not play effective role to circumvent sudden failure. Although the confinement effects on reduction of damage sensitively and experimentally seems obvious, but quantifying it to evaluate damage index has not been done before. In this paper the numerical changes in damage index in accordance with confinement ratio has been represented.

3. Basically damage index is defined to predict vulnerability of structures under critical states such as severe earthquake and high axial load. But  $DI_{PA}$  only calculate damage index when maximum rotation is attained. So, the damage index needs a modification to consider responses in presence of axial force. As the results of analyses show the modified index is capable to determine damage when axial load minimizes the deformation and energy capacity of section. This capability of modified damage index mainly owes to used fiber method that considers interaction of axial load and flexural moment and distribution of plasticity. The comparison between the result of modified damage index and other counterparts demonstrates more reliable evaluation of damage index.

## References

- [1] ASCE, Seismic rehabilitation of existing buildings. Virginia: American Society of Civil Engineers, 2006.
- [2] Behnam, B, Sebt, M.H., Vosoughifar, H.M.:2006, Evaluating Quality Seismic damage index for Urban Residential Buildings, International Journal of Civil Engineering(IJCE), 4(2).
- [3] Sadrnejad, S.A, Labizadeh, M.:2006, A continuum/discontinuum micro plane damage model for concrete , International Journal of Civil Engineering (IJCE), 4(4).
- [4] Krawinkler, H, Zohrei, M.:1983, Cumulative damage in steel structures subjected to earthquake ground motions, Computers and Structures, 16(1-4): 531-541.
- [5] Dipasquale, E, Cakmak, A. S.:1990, Seismic damage assessment using linear models, Soil Dynamics and Earthquake Engineering, 9(4): 194-215.
- [6] Powell, G. H., Allahabadi, R.: 1988, Seismic damage prediction by deterministic methods: concepts and procedures, Earthquake Engineering and Structural Dynamics, 16(5): 719-734.
- [7] Cosenza, E, Manfredi, G, Ramasco, R.:1988, The use of damage functionals in earthquake engineering: a comparison between different methods, Earthquake Engineering and Structural Dynamics, 22(10): 855-868.
- [8] Omid, O, Lotfi, V.:2010, Finite element analysis of concrete structures using plastic-damage model in 3-D implementation, International Journal of Civil Engineering(IJCE), 8(3)
- [9] Dipasquale, E., Cakmak, A. S.:1989, On the relation between local and global damage indices, Technical Report No. NCEER-89/34, National Centre for Earthquake Engineering Research, State University of New York at Buffalo, NY.
- [10] Fajfar, P.:1992 Equivalent ductility factors taking into account low cycle fatigue, Earthquake Engineering and Structural Dynamics, 21(10): 837-848.
- [11] Park, Y. J., Ang, A. H. S.:1985, Mechanistic seismic damage model for reinforced concrete, Journal of Structural Division (ASCE), 111(4): 722-739.
- [12] Reinhorn, A. M., and Valles, R. E.:1995, Damage evaluation in inelastic response of structures: a deterministic approach, Report No. NCEER-95-xxxx, National Centre for Earthquake Engineering Research, State University of New York at Buffalo.
- [13] Colombo, A., Negro, P.:2005, A damage index of generalized applicability, Engineering Structures, 27(88): 1164-1174.
- [14] Kono, S., Watanabe, F.:2000, Damage evaluation of reinforced concrete columns under multi-axial cyclic loadings, The Second U.S.-Japan Workshop on Performance-Based Earthquake Engineering Methodology for Reinforced Concrete Building Structures. Sapporo, Hokkaido, Japan, 11-13 Sep.
- [15] Chen, W. F., Duan, L.:2003, Bridge engineering seismic design. CRC Press, Boca Raton, London New York Washington DC.
- [16] Spacone, E., Filippou, F.C., Taucer, F.F.:1996, Fiber beam-column element for nonlinear analysis of R/C frames. Part I: Formulation, Earthquake Engineering and Structural Dynamics, 25(7): 711-725.
- [17] de Souza, R.M.:2000, Force-based finite element for large displacement inelastic analysis of frames, Ph.D. dissertation, Department of Civil and Environmental Engineering, University of California, Berkeley.
- [18] Tsuchiya, S., Maekawa, K.: 2006, Cross-sectional damage index for RC beam-column members subjected to multi-axial flexure, Journal of Advanced Concrete Technology, 4(1): 179-192.
- [19] Hognestad, E.: 1951, A study of combined bending and axial load in reinforced concrete members. University of Illinois Engineering Experimental Station, Bulletin Series No. 399, Urbana, IL, Nov.
- [20] Kent, D.C., Park, R.:1971, Flexural members with confined concrete. Journal of Structural Division (ASCE), 97(ST7): 1969-1990.
- [21] Hoshikuma, J., Kawashima, K., Nagaya, K., Taylor, A.W.:1997, Stress-Strain Model for Confined Reinforced Concrete in Bridge Piers. Journal of Structural Engineering (ASCE), 123(5): 624-633.
- [22] Mander, J.B., Priestley, M.J.N., Park, R.:1988, Theoretical stress-strain model for confined concrete, Journal of Structural Engineering (ASCE), 114(8): 1804-1826.
- [23] Antoniou, S., Pinho, R.:2005, SeismoStruct, www.seismosoft.com, March.
- [24] Kunnath, S. K., Reinhorn, A. M., Lobo, R. F.:1992, IDARC version 4.0: a program for the inelastic damage analysis of reinforced concrete structures, Technical Report No. NCEER-92/22, National Centre for Earthquake Engineering Research, State University of New York at Buffalo, NY.

- [25] Menegotto, M., Pinto, P.E.:1973, Method of analysis for cyclically loaded RC plane frames including changes in geometry and non-elastic behaviour of elements under combined normal force and bending. Symposium on the Resistance and Ultimate Deformability of Structures Acted on by Well Defined Repeated Loads, International Association for Bridge and Structural Engineering, Zurich, Switzerland, 15-22.
- [25] Dipasquale, E., Cakmak, A.S.:1988, Identification of the serviceability limit state and detection of seismic structural damage. Technical Report NCEER-88/22, National Centre for Earthquake Engineering Research, State University of New York at Buffalo, NY.
- [27] Priestley, M.J.N., Seible, F., Calvi, G.M.:1996, Seismic design and retrofit of bridges, John Wiley & Sons, New York.